POLITECNICO DI TORINO
Repository ISTITUZIONALE

# Molecular dynamics, quantum mechanical and semi-empirical investigations of paclitaxel-containing oil-in-water pluronic F127 and lignin microemulsions

*Original*
Molecular dynamics, quantum mechanical and semi-empirical investigations of paclitaxel-containing oil-in-water pluronic F127 and lignin microemulsions / Karimi, P., Poorsargol, M., Rahdar, A., Baino, F.. - In: NANO TRENDS. - ISSN 2666-9781. - 11:(2025). [10.1016/j.nwnano.2025.100137]

*Availability:*
This version is available at: 11583/3005907 since: 2025-12-16T11:09:51Z

*Publisher:*
Elsevier

*Published*
DOI:10.1016/j.nwnano.2025.100137

*Terms of use:*

This article is made available under terms and conditions as specified in the corresponding bibliographic description in the repository

*Publisher copyright*

(Article begins on next page)

07 September 2026

Nano Trends 11 (2025) 100137

Contents lists available at ScienceDirect

Nano Trends

journal homepage: www.elsevier.com/locate/nantre

# Molecular dynamics, quantum mechanical and semi-empirical investigations of paclitaxel-containing oil-in-water pluronic F127 and lignin microemulsions

Pouya Karimi [a,*], Mahdiye Poorsargol [a], Abbas Rahdar [b], Francesco Baino [c,*]

[a] Department of Chemistry, Faculty of Sciences, University of Zabol, Zabol, Iran
[b] Department of Physics, School of Basic Sciences, University of Zabol, Zabol, Iran
[c] Institute of Materials Physics and Engineering, Department of Applied Science and Technology, Politecnico di Torino, Torino, Italy

ARTICLE INFO

*Keywords:*
Paclitaxel
F127, Lignin
Exchange interaction
Microemulsion

ABSTRACT

Oil-in-water microemulsions based on surfactants F127 and lignin may enhance the availability of Paclitaxel (PTX) in bio-systems that lead to improved drug delivery. Therefore, PTX-loaded microemulsions were designed by means of molecular dynamics (MD) simulations, density functional theory (DFT), and semi-empirical methods. The MD simulations revealed a more stable release of PTX in microemulsion form compared to the bulk one (free drug). Quantum mechanics calculations pointed out that stability of the PTX-F127 microemulsions are higher compared to PTX-Lignin ones. Furthermore, hydrogen bond (HB) forces help to ensure the stability of the PTX-surfactants in microemulsions. Alteration of atomic charges due to hydrogen bond forces and charge transport (CT) influence the stability of the PTX-loaded microemulsions. HB interactions appeared to play an important role on the improved action of PTX in microemulsion systems compared to free drug. The delivery of PTX in microemulsion systems is attributable to the exchange interactions between surfactants and PTX. The semi-empirical calculations showed that the heat of formation values ($\Delta H_f$) of the PTX-F127 complexes are larger (more negative) than those for the PTX-Lignin ones.

## 1. Introduction

Paclitaxel (PTX) is a member of the family of taxanes with lipophilic nature that acts as chemotherapeutic agent [1]. This drug has been used for treating breast, lung, and ovarian cancers [2]. However, PTX has poor bioavailability [3] as a result of its low solubility in biological environment [4]. Thus, it is necessary to increase solubility of this drug. Formerly, drug carriers were proposed for this purpose [5–8].

Oil-in-water microemulsions based on surfactants are excellent systems that help the release of hydrophobic drugs as a result of high bioavailability and small toxic effects [9–13]. It should be noted that Pluronic (non-ionic) surfactants are better in oil-in-water microemulsions than ionic ones owing to higher stability and less toxicity [14]. Permeability and oral absorption of PTX are enhanced by inclusion of drug into microemulsions [15,16].

Copolymers may occasionally exhibit toxic effects depending on their composition and how they interplay with biological systems. Thus, such copolymers can harm or kill cells. In contrast, some copolymers such as (poly(ethylene oxide)−poly(propylene oxide)− poly(ethylene oxide) [17] with small toxic effects act as good steady factors in oil-in-water microemulsion systems and have good ability to encapsulate the hydrophobic drugs. F127 is a functional copolymer and good material for encapsulation [18]. The potential of F127 was formerly considered in systems containing hydrophobic drugs [19–23]. Additionally, lignin is a safe surfactant that has already been proposed for biomedical applications [24,25], with special focus on the better release of drugs [26,27]. Microemulsions that include lignin have been previously utilized as suitable transporters with enhanced effectiveness [28–30]. Thus, on the basis of the previous literature, we used F127 and lignin in the current work as safe surfactants in the delivery process of PTX.

Experiments regarding drug release based on microemulsions offer promising results. However, analysis of molecular interactions is difficult using such examinations. Instead, MD simulations and computational quantum mechanical methods give useful results about the mentioned interactions [22,23]. In fact, computational researches

* Corresponding authors.
*E-mail addresses:* pkarimi@uoz.ac.ir (P. Karimi), poorsargol.m@uoz.ac.ir (M. Poorsargol), a.rahdar@uoz.ac.ir (A. Rahdar), francesco.baino@polito.it (F. Baino).

https://doi.org/10.1016/j.nwnano.2025.100137
Received 29 November 2024; Received in revised form 5 August 2025; Accepted 7 August 2025
Available online 8 August 2025
2666-9781/© 2025 The Authors. Published by Elsevier Ltd. This is an open access article under the CC BY license (http://creativecommons.org/licenses/by/4.0/).

accompany experimental ones. In the current work, interplays between PTX and F127/ lignin are studied using MD simulations, quantum mechanical and semi-empirical calculations to gain a more complete knowledge about the characteristics of the interactions between PTX and the surfactants. Hydrogen bond analysis, radial distribution function curves, molecular structures, energies, bond lengths, charge transport (CT), electron charge density values and related properties, donor-acceptor interaction energies, and energy decomposition analyses (EDA) were considered to discover factors that have a role in stability of the complexes. Experimental designs, mainly in clinical trials, depend on theoretical principles to confirm valid and reliable results. We hope that theoretical results of the present study regarding strength and nature of the interactions between PTX and surfactants would be useful for future experimental designs and clinical applications.

## 2. Methods

### 2.1. Simulation methodology

MD has been used as a simulation technique to design PTX-F127 and PTX-lignin microemulsions as well as to compare the results with the behavior of free PTX in bulk form. The bulk form includes 15 PTX molecules and 15 free radicals of 2,2-diphenyl-1-picrylhydrazyl (DPPH), dispersed randomly using PACKMOL in a box containing methanol [31]. PTX-F127 and PTX-Lignin microemulsions were also made using PACKMOL software. For this purpose, first, 15 molecules of PTX were randomly placed in ethyl butyrate. Then, the sides were covered with the desired surfactant (F127 or Lignin). Finally, the desired microemulsion was placed in a box containing methanol and DPPH. Automated Topology Builder (ATB) was used to generate topology and conformation of these structures [32]. The GROMOS 54 A7 force field was selected to represent all bonded and nonbonded interactions [33]. Long-range electrostatic interactions were calculated using the particle mesh Ewald (PME) method [34]. The cut-off distance for the van der Waals interactions was taken as 1.2 nm. Before starting MD simulation, energy minimization was carried out using the steepest descent method. Afterwards, the system went through NVT ensemble MD simulation at constant temperature of 298 K for 200 ps and then continued employing NPT ensemble for 400 ps at a constant temperature of 298 K and constant pressure of 1 bar by using V-rescale thermostat and Parrinello–Rahman barostat [35,36]. MD simulation was performed NPT for 50 ns and the used integration time step in the MD simulation was 2 fs. Equations of motion were integrated using the Verlet algorithm. Periodic boundary conditions were used in all three directions and the trajectories, velocities and forces on the constituent atoms of the system were stored at 40 ps intervals. MD simulations were performed using GROMACS version 2022.3 [37].

### 2.2. Quantum mechanics

Molecular structures of PTX, F127, lignin, and all drug-surfactant systems were optimized at the B3LYP/6–31G(d,p) level by means of Gaussian09 program [38]. Interaction energy of a binary complex AB was calculated as:

$$\Delta E = E_{AB} - -(E_A + E_B) \quad (1)$$

In the Eq. (1), A and B refer to drug and surfactant, respectively.

The electron charge density values have been estimated through atoms in molecules (AIM) technique by AIM2000 software [39]. The interactions between molecular orbitals were carried out using natural bond orbital (NBO) scheme [40] by means of NBO program [41]. The NBO method estimates charge transports between molecular orbitals. The second-order perturbation theory was the way for specification of the energetic weights of these molecular orbitals. Stabilizing energy ($E^{(2)}$) in each donor–acceptor interaction was measured by an operator (Fock) for donor and acceptor orbitals (φi and φj) as:

$$E^{(2)} = \frac{|<\varphi i|_F^{|\varphi j>|}2}{\varepsilon i - \varepsilon j} \quad (2)$$

In this equation, εi and εj are Eigenvalues related to the φi and φj, respectively.

Semi-empirical techniques were implemented to include all thermochemistry improvements to eventually gain the heat of formations. Thus, these calculations were performed using AM1 method [42] to better study hydrogen bond interplays.

## 3. Results and discussion

### 3.1. MD simulation

First, the equilibrium of the simulated systems was considered. The root mean square deviation (RMSD) was analyzed to investigate the equilibrium of the systems during the structural changes. Then, the number of HB interactions between these molecules was analyzed in three systems: bulk, PTX-F127 microemulsion, and PTX-Lignin microemulsion to further investigate the interactions between PTX and DPPH molecules. Moreover, the mean electrostatic energy ($E_{el}$) and Lennard-Jones energy ($E_{L\text{-}J}$) values between PTX, F127, lignin, and DPPH in the three systems (bulk, PTX-F127, and PTX-Lignin) were calculated. Finally, radial distribution functions (RDFs, g(r)) for PTX-F127 and PTX-Lignin systems were plotted.

#### 3.1.1. RMSD curves

RMSD curves are plotted for the total system as a function of simulation time in Fig. 1, which shows RMSD curves for three simulated systems: bulk, PTX-F127 and PTX-Lignin systems. Fig. 1 demonstrates that the RMSD curve in the bulk system flattens after 2 ns, at which time the system reaches equilibrium. Due to the complexity of microemulsions, the deviations of the RMSD curves are higher in PTX-F127 and PTX-lignin systems, which reach equilibrium after about 10 ns. As the bulk system is stabilized faster, it can be argued that PTX interacts with DPPH faster and more easily in this system. Meanwhile, there is a lower probability of PTX interaction with DPPH in microemulsions due to the presence of F127 and lignin surfactants.

#### 3.1.2. Assessment of number of HBs

Fig. 2 depicts the number of HBs formed between PTX and DPPH in the simulated systems according to simulation time. Based on Fig. 2, the number of HBs formed between PTX and DPPH is very high in the bulk system, indicating maximal interaction between PTX and DPPH. In the bulk system, the mean number of HBs during simulation has been calculated as 0.78; on the contrary, as shown in Fig. 2, the number of HBs formed between PTX and DPPH is much lower in PTX-F127 and PTX-Lignin microemulsions, suggesting minimal interaction between PTX and DPPH in these systems. The mean number of HBs for PTX-F127 and PTX-Lignin systems is 0.05 and 0.16, respectively. The small number of HBs in microemulsions suggests the absence of PTX around DPPH. The mean number of HBs between PTX and surfactants including F127 and lignin in PTX-F127 and PTX-Lignin microemulsions was calculated as 1.51 and 1.59, respectively, which is much higher than DPPH. Therefore, it can be argued that the formation of HBs between PTX and surfactants has made these microemulsions stable.

#### 3.1.3. Energy analysis

The $E_{el}$ and $E_{L\text{-}J}$ values between PTX, F127, lignin, and DPPH in the three systems (bulk, PTX-F127, and PTX-Lignin) were calculated along with the simulation and are presented in Table 1. The comparison of l-J and electrostatic energies in Table 1 shows that van der Waals forces play a considerable role in the PTX-DPPH interaction. The $E_{L\text{-}J}$ value between PTX and DPPH in the bulk system equals to $-29.66$ kcal mol$^{-1}$. This value is indicative of a strong interaction. On the contrary, this

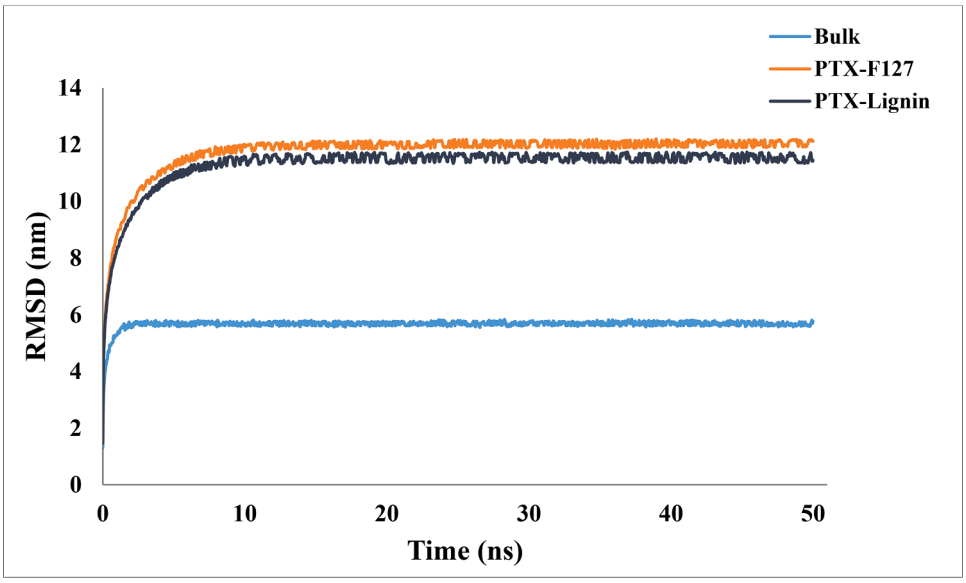


**Fig. 1.** RMSD curves of total system for three simulated systems: bulk, PTX-F127 and PTX-Lignin microemulsions as a function of the simulation time.

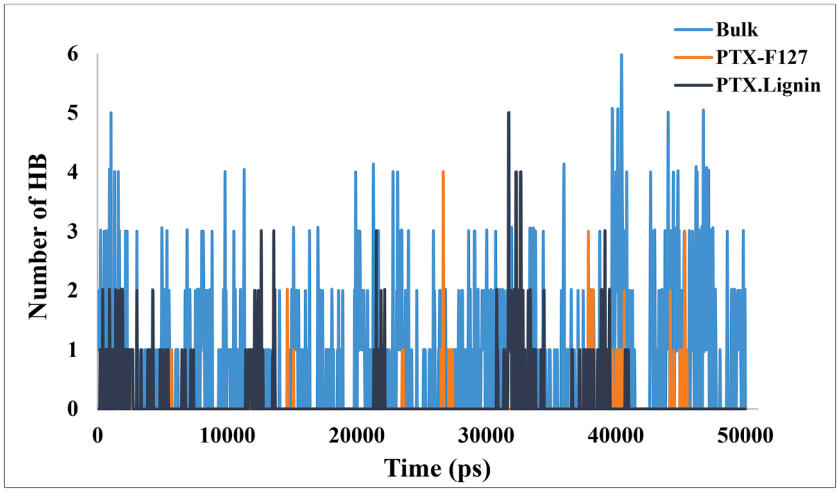


**Fig. 2.** The number of HBs formed between PTX and DPPH in the simulated systems according to simulation time.

**Table 1**
The mean electrostatic and Lennard-Jones energies between the different groups, including PTX, DPPH, F127, and Lignin (kcal $mol^{-1}$).

| System | $E_{el}$ | $E_{L\text{-}J}$ |
|---|---|---|
| PTX-F127 (micro-F127) | −8.41 | −166.35 |
| PTX-Lignin (micro-Lignin) | −3.06 | −15.60 |
| PTX-DPPH (bulk) | −5.74 | −29.66 |
| PTX-DPPH (micro-F127) | −0.42 | −2.25 |
| PTX-DPPH (micro-Lignin) | −1.27 | −6.54 |

Terminology: $E_{el}$ = Electrostatic energy; $E_{L\text{-}J}$ = Lennard-Jones energy.

energy dropped to −2.25 and −6.54 kcal $mol^{-1}$ in PTX-F127 and PTX-Lignin microemulsions, respectively. This result suggests the significant reduction of interactions between PTX and DPPH in microemulsions. This observation aligns with the above-mentioned findings, which show maximal interaction between PTX and DPPH in bulk system and minimal interaction between PTX and DPPH in microemulsions. Furthermore, the values of electrostatic and l-J energies between PTX and F127 and lignin surfactants were also calculated in systems containing microemulsion. Similarly, the results suggest that van der Waals interactions play a key role in the interplay between PTX and surfactants. Thus, in these microemulsions, PTX interacts with F127 and lignin surfactants, decreasing the speed of PTX release from the microemulsion and ensuring the stable delivery of the drug to the target tissues.

Moreover, the comparison of the energy values shows that the l-J energy between PTX and the F127 surfactant is much higher than that between PTX and the lignin surfactant, suggesting a much stronger interaction between PTX and F127 surfactant. It was previously observed that phenytoin (PHT) has a stronger interaction with F127, and its release rate from F127/PHT nanomicelles was lower than Lignin/PHT nanomicelles [43].

### *3.1.4. Presentation of RDF curves*

RDFs can provide more structural insight into the interactions existing within PTX-F127 and PTX-Lignin microemulsions. Fig. 3 shows the RDFs. The g(r) value for the F127 surfactant shows that the distribution of F127 molecules around PTX is much higher. The g(r) value for the lignin surfactant is lower, suggesting the small distribution of lignin molecules around PTX. Consequently, the greater distribution of F127 molecules around PTX indicates the stronger interaction between PTX and F127. The stronger interaction of PTX with F127 can cause further

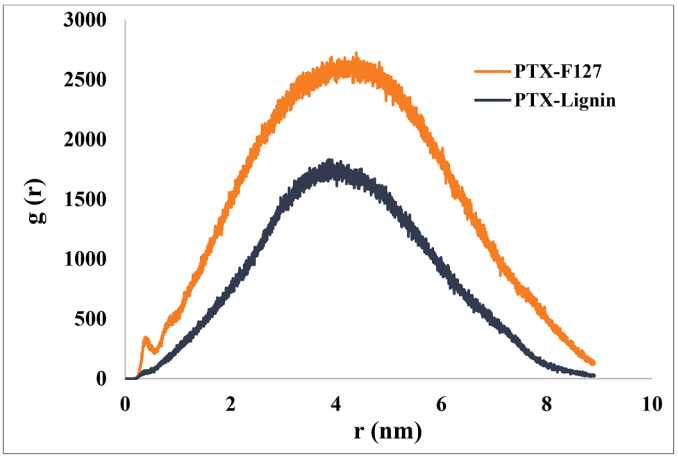


**Fig. 3.** Radial distribution function (g(r)) of F127 or Lignin surfactants around PTX for PTX-F127 and PTX-Lignin microemulsions.

loading of PTX in the PTX-F127 microemulsion. Higher drug loading in microemulsions significantly increases the bioavailability of the drug. Besides, the stronger interaction of the drug with F127 surfactant leads to a slower release of the drug from the microemulsion and ensures a more stable delivery of PTX in the target tissues.

### 3.2. Quantum mechanics calculations

First, energy data and formation of HB interactions between carriers and PTX were studied. Then, changes of charges on atoms that contribute in HB interactions were considered. Specifically, charge transfers, electron charge densities and related properties were examined. Lastly, decomposition of interaction energies was investigated.

#### 3.2.1. Energy data

PTX is a chemotherapy medicine that used for treatment of various cancers [44]. The chemical structure of PTX is displayed in Fig. 4.

It appears that formations of hydrogen bond interplays between carriers and PTX influence the effectiveness of drug release progression. Molecular geometries of PTX-F127 and PTX-Lignin systems have been optimized via Gaussian09 program package. As shown in Fig. 5, these complexes are made by way of intermolecular hydrogen bond interplays between surfactants (as HB donors) and PTX (as HB acceptor). Contributing atoms in the mentioned interactions are denoted as $O_a$, $H_b$, and $O_c$. Energy data and binding energy (-ΔE) values of the complexes are collected in Table 2.

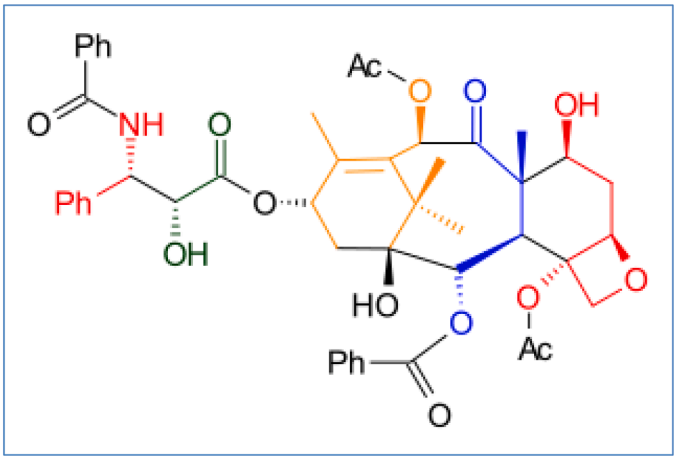


**Fig. 4.** Typical structure of Paclitaxel.

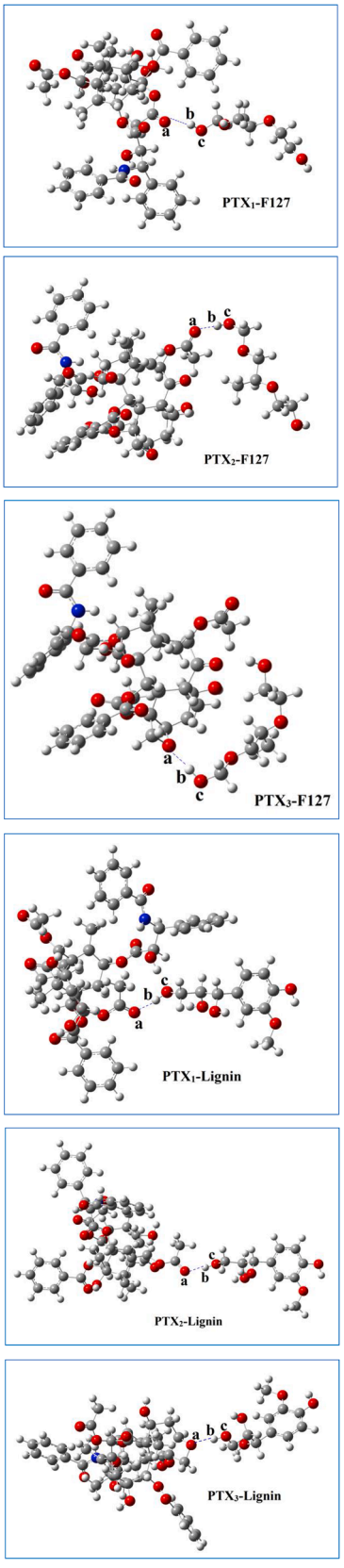


**Fig. 5.** The binary systems containing PTX and surfactants.

**Table 2**
Electronic data (in eV) and binding energy values (in kcal $mol^{-1}$) of the complexes.

| | $E_{HOMO}$ | $E_{LUMO}$ | $\Delta E_{L\text{-}H}$ | -ΔE |
|---|---|---|---|---|
| $PTX_1$-F127 | −5.242 | −1.437 | 3.805 | 7.56 |
| $PTX_2$-F127 | −5.258 | −1.415 | 3.843 | 10.67 |
| $PTX_3$-F127 | −5.267 | −1.443 | 3.824 | 12.82 |
| $PTX_1$-Lignin | −5.199 | −1.436 | 3.763 | 12.84 |
| $PTX_2$-Lignin | −5.265 | −1.421 | 3.844 | 5.28 |
| $PTX_3$-Lignin | −5.243 | −1.443 | 3.800 | 4.13 |

Terminology: $E_{HOMO}$ = Energy of highest occupied molecular orbital; $E_{LUMO}$ = Energy of lowest unoccupied molecular orbital; $\Delta E_{L\text{-}H}$ = Energy gap; -ΔE = Binding energy.

Results indicate that the sum of binding energy values of the PTX-F127 systems is higher with respect to the PTX-Lignin systems. Therefore, F127 forms stronger HB interactions with PTX than lignin. Energies of the highest occupied molecular orbital (HOMO) and lowest unoccupied molecular orbital (LUMO) and the gap between $E_{HOMO}$ and $E_{LUMO}$ ($\Delta E_{L\text{-}H}$) of the mentioned systems are also gathered in Table 2. The $E_{HOMO}$ and $E_{LUMO}$ of the free PTX are −5.230 and −1.409 eV, respectively.

The differences between $E_{HOMO}$ values of the PTX-F127 systems and $E_{HOMO}$ of free PTX are lesser than the PTX-Lignin systems. The same result is also obtained in the case of $E_{LUMO}$ values. It seems that these differences influence the magnitude of BE values of the complexes. Indeed, sum of $E_{LUMO}$ values of both complexes is the same. However, sum of $E_{HOMO}$ for the PTX-F127 systems is larger (more negative) with respect to the PTX-Lignin systems. As a result, the higher stability of the PTX-F127 complexes can be attributed to the levels of HOMO of these structures.

### 3.2.2. Charge of atoms

Charges in the free PTX, surfactants, and corresponding binary systems were studied to investigate the relationship between binding energy values of the complexes and atomic charges. Charge transport (CT) in the binary systems and charges of the atoms that play a role in the hydrogen bond interplays are presented in Table 3.

Results suggest that there is a linear relationship between changes of |CT| and binding energies the complexes. Increase of |CT| leads to increase of binding energy values of the PTX-F127 complexes (Fig. 6a), but the reverse is true in the case of PTX-Lignin ones (Fig. 6b). Thus, CT that occurred between PTX and surfactants is an important factor that dictates BE values of the resulting complexes.

PTX interplays with both F127 and lignin through three positions that are denoted with $O_a$ in all complexes. Charges of these positions before interactions with surfactants are −0.501, −0.492, and −0.553 e, respectively. Also, charge of atom $H_b$ in the free F127 and lignin is 0.336 and 0.338 e, respectively. Moreover, charge of $O_c$ in the free F127 and lignin is −0.565 and −0.578 e, respectively. Results specify that formation of complexes is followed by decrease of charge of atoms $O_a$ and $O_c$. However, charge of $H_b$ increases in the binary systems in comparison to free surfactants. Absolute changes of $q_{Oa}$, $q_{Hb}$, and $q_{Oc}$ owing to HB interactions, namely $|\Delta q_{Oa}|$, $|\Delta q_{Hb}|$, and $|\Delta q_{Oc}|$ are also presented in Table 3. It seems that these descriptors have an effect on the BE values. In fact, increase of $|\Delta q_{Hb}|$ and $|\Delta q_{Oc}|$ is accompanied by increase of binding energy values of the PTX-F127 and PTX-Lignin systems. However, increase of $|\Delta q_{Oa}|$ is pursued by increase of binding energy values of the PTX-F127 systems and the inverse is true for the PTX-Lignin systems. Actually, alteration of the binding values of the complexes with $|\Delta q_{Oa}|$ is the same as with |CT|. Consequently, changes of atomic charges of HB donors on account of HB interactions have an imperative role on the strength of these binary systems.

### 3.2.3. NBO and AIM analyses

The NBO surveys were performed to obtain $E^{(2)}$ values associated to charge transports between orbitals of PTX and surfactants. Results show that charge transports occur from $Lp_{(Oa)}$ to $\sigma^*_{(Hb-Oc)}$ in both binary systems. The $E^{(2)}$ value for the mentioned interaction in the $PTX_1$-F127, $PTX_2$-F127 and $PTX_3$-F127 is 3.66, 3.95, and 7.25 kcal $mol^{-1}$, respectively. Also, the corresponding $E^{(2)}$ value in the $PTX_1$-Lignin, $PTX_2$-Lignin and $PTX_3$- Lignin is 5.75, 3.97, and 5.05 kcal $mol^{-1}$, respectively. Sum of stabilizing energy ($\sum E^{(2)}$) values for above electron charge transports in the PTX-F127 complexes is slightly larger than that for the PTX-Lignin ones. Also, complexes with larger $E^{(2)}$ values have relatively superior BE values. Thus, donor-acceptor interplays can influence on strength of interactions in the mentioned binary systems.

AIM calculations were performed to discern the relation between electron charge density values (and related properties) and binding energies. Electron charge density at HB critical point ($\rho_{HBCP}$) that made between PTX and surfactants and related properties are collected in Table 4. Results show that complexes with larger binding energy values have relatively larger $\rho_{HBCP}$ values. In addition, Laplacian of electron charge density ($\nabla^2\rho$), kinetic electronic energy density (G), potential electronic energy density (V), and second Eigenvalue of Hessian matrix ($\lambda_2$) were calculated and given in Table 4, too.

The $\nabla^2\rho$ values related to the PTX-Lignin systems are smaller with respect to the PTX-F127 ones. The $(\rho(r)\lambda_2)$ for binary systems in the current work is less than zero. This outcome shows that the character of the HB interplays in these systems is attractive. Also, sum of V and G in both complexes is negative. In fact, there are accumulations of electron charges in paths of HB interactions. Seemingly, orientation of PTX near each surfactant is important in distribution of electron charges and influences the strength of HB interaction.

### 3.2.4. Energy decomposition study

The localized molecular orbital energy decomposition analyses (LMO-EDA) [45] have been performed on the hydrogen bonded molecular systems to classify the various components of interaction energies of the binary systems. Interaction energy comprises electrostatic, exchange, repulsion, and polarization energies that are represented as $E_{es}$, $E_{ex}$, $E_{repul}$ and $E_{polar}$, respectively. These components are collected in Table 5. As can be observed, $E_{ex}$ is the most significant component of interaction energy in all cases. Thus, $E_{ex}$ has a good contribution in the stability of the complexes.

The correlation between the $d_{HB}$ and $E_{ex}$ values is represented in

**Table 3**
Magnitudes of charge transports, charge of most important atoms and absolute changes of atomic charges during HB interactions.

| |CT| | $q_{Oa}$ | $q_{Hb}$ | $q_{Oc}$ | $\lvert\Delta q_{Oa}\rvert$ | $\lvert\Delta q_{Hb}\rvert$ | $\lvert\Delta q_{Oc}\rvert$ |
|---|---|---|---|---|---|---|---|
| $PTX_1$-F127 | 0.0427 | −0.5122 | 0.3374 | −0.578 | 0.1154 | 0.0139 | 0.1321 |
| $PTX_2$-F127 | 0.0507 | −0.5033 | 0.3461 | −0.586 | 0.1153 | 0.1014 | 0.2060 |
| $PTX_3$-F127 | 0.0738 | −0.568 | 0.3433 | −0.586 | 0.1546 | 0.1014 | 0.2072 |
| $PTX_1$-Lignin | 0.0043 | −0.5094 | 0.3679 | −0.616 | 0.0874 | 0.3029 | 0.3766 |
| $PTX_2$-Lignin | 0.0513 | −0.5032 | 0.3521 | −0.607 | 0.1142 | 0.1448 | 0.2817 |
| $PTX_3$-Lignin | 0.0620 | −0.5654 | 0.3484 | −0.61 | 0.1285 | 0.1082 | 0.3162 |

Terminology: |CT| = Charge transport; $q_{Oa}$ = Charge of hydrogen bond acceptor atom; $q_{Hb}$ = Charge of hydrogen atom; $q_{Oc}$ = Charge of hydrogen bond donor atom; $|\Delta q_{Oa}|$ = Change of charge on hydrogen bond acceptor atom due to HB interaction; $|\Delta q_{Hb}|$ = Change of charge on hydrogen atom due to HB interaction; $|\Delta q_{Oc}|$ = Change of charge on hydrogen bond donor atom due to HB interaction.

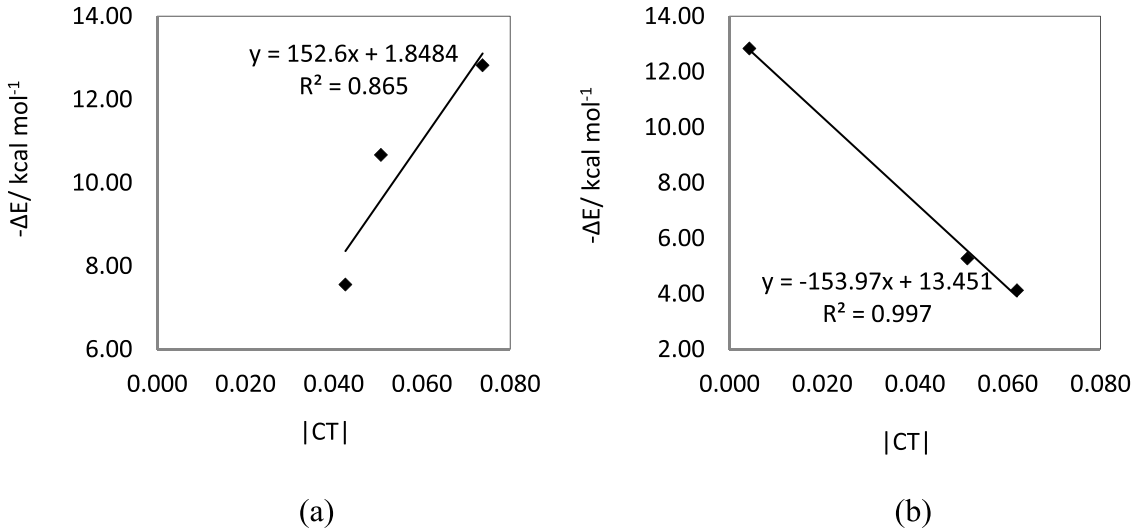


**Fig. 6.** Correlation between magnitude of charge transport and BE values of (a) PTX-F127 and (b) PTX-Lignin complexes.

**Table 4**
Electron charge density values and associated properties at HB critical points in the binary systems (au).

| $\rho_{HBCP}$ | | $\nabla^2\rho$ | G | V | $\lambda_2$ | G/\|V\| |
|---|---|---|---|---|---|---|
| $PTX_1$-F127 | 0.0281 | −0.0258 | 0.0285 | −0.0312 | −0.0431 | 0.914 |
| $PTX_2$-F127 | 0.0400 | −0.0268 | 0.0366 | −0.0464 | −0.0660 | 0.789 |
| $PTX_3$-F127 | 0.0340 | −0.0266 | 0.0329 | −0.0392 | −0.0546 | 0.840 |
| $PTX_1$-Lignin | 0.0467 | −0.0274 | 0.0412 | −0.0551 | −0.0790 | 0.749 |
| $PTX_2$-Lignin | 0.0405 | −0.0269 | 0.0370 | −0.0471 | −0.0670 | 0.786 |
| $PTX_3$-Lignin | 0.0388 | −0.0269 | 0.0362 | −0.0455 | −0.0641 | 0.796 |

Terminology: $\rho_{HBCP}$ = Electron charge density at hydrogen bond critical point; $\nabla^2\rho$ = Laplacian of electron charge density; $G$ = Kinetic electronic energy density; $V$ = Potential electronic energy density; $\lambda_2$ = Second eigenvalue of Hessian matrix; G/|V| = Ratio of kinetic to potential electronic energy density.

**Table 5**
Different parts of interaction energies for the binary systems (in kcal $mol^{-1}$).

| $E_{es}$ | | $E_{ex}$ | $E_{repul}$ | $E_{polar}$ |
|---|---|---|---|---|
| $PTX_1$-F127 | −7.71 | −7.98 | 14.77 | −1.79 |
| $PTX_2$-F127 | −13.90 | −15.29 | 28.55 | −3.13 |
| $PTX_3$-F127 | −12.48 | −12.78 | 23.70 | −3.11 |
| $PTX_1$-Lignin | −31.18 | −40.31 | 75.52 | −9.60 |
| $PTX_2$-Lignin | −14.37 | −15.52 | 28.90 | −3.32 |
| $PTX_3$-Lignin | −12.48 | −12.78 | 23.70 | −3.11 |

Terminology: $E_{es}$ = Electrostatic energy; $E_{ex}$ = Exchange energy; $E_{repul}$ = Repulsion energy;.
$E_{polar}$ = Polarization energy.

equation 3. A linear relationship was found with $R^2 = 0.72$. In fact, the complexes with more negative exchange energies encompass smaller $d_{HB}$ values. $d_{HB} = 0.005\ E_{ex} + 1.91$ (3)

Therefore, exchange interaction has an essential part on the strength of the intermolecular hydrogen bond interplay within each of PTX-F127 and PTX-Lignin binary systems.

### 3.3. Semi-empirical computations

Some methods include parameters that cover all thermochemistry correction factors. If truth be told, these techniques utilize empirical corrections to raise the performance of calculations. Thus, AM1 method was used to calculate heat of formation ($\Delta H_f$) values of the binary systems. The $\Delta H_f$ values for $PTX_1$-F127, $PTX_2$-F127, $PTX_3$-F127, $PTX_1$-Lignin, $PTX_2$-Lignin, and $PTX_3$-Lignin are −621.802, −621.128, −622.228, −625.888, −620.471, and −612.610 kcal $mol^{-1}$, respectively. Results indicate that sum of $\Delta H_f$ values of the PTX-F127 systems are more negative than the PTX-Lignin. As said, sum of binding energy values of the PTX-F127 systems are larger than the PTX-Lignin. It seems that there is a relation between stability of the binary systems and $\Delta H_f$ values. Outcomes demonstrate that systems with larger binding energy values have fairly more negative $\Delta H_f$ values.

Finally, the most important quantitative findings of the present study are reported in Table 6.

## 4. Conclusions

In this work, microemulsions based on F127 and lignin surfactants were investigated using MD simulations and DFT study. The MD simulations revealed the more stable release of PTX in microemulsion form than in bulk. Also, strong interactions between PTX and the F127 were observed in the PTX-F127 microemulsion. Results of quantum mechanical studies indicate that the BE values of the PTX-F127 systems are larger than PTX-Lignin structures. There are linear correlations between magnitudes of charge transports and BE values. Levels of the highest occupied molecular orbitals of the PTX-F127 systems are lower than the PTX-lignin structures. Alterations of charges of oxygen atoms as HB

**Table 6**
Comparative summary table about the interactions in PTX-F127 and PTX-Lignin.

| Parameters | PTX-F127 | PTX-Lignin |
|---|---|---|
| Mean number of HBs | [1] $n_{HBs} = 1.51$ | $n_{HBs} = 1.59$ |
| Electrostatic energy | [2] $E_{el} = -8.41$ kcal $mol^{-1}$ | $E_{el} = -3.06$ kcal $mol^{-1}$ |
| Lennard-Jones energy | [3] $E_{L\text{-}J} = -166.35$ kcal $mol^{-1}$ | $E_{L\text{-}J} = -15.60$ kcal $mol^{-1}$ |
| Sum of interaction energies | [4] $\sum\Delta E = -31.05$ kcal $mol^{-1}$ | $\sum\Delta E = -22.25$ kcal $mol^{-1}$ |
| Sum of change of charge on the $O_a$ atom | [5] $\sum\Delta q_{Oa} = -0.039$ e | $\sum\Delta q_{Oa} = -0.033$ e |
| Sum of change of charge on the $H_b$ atom | [6] $\sum\Delta q_{Hb} = 0.022$ e | $\sum\Delta q_{Hb} = 0.056$ e |
| Sum of change of charge on the $O_c$ atom | [7] $\sum\Delta q_{Oc} = -0.055$ e | $\sum\Delta q_{Oc} = -0.097$ e |
| Sum of absolute value of charge transfer | [8] $\sum\|CT\| = 0.167$ e | $\sum\|CT\| = 0.118$ e |
| Sum of stabilizing energy | [9] $\sum E^{(2)} = 14.86$ kcal $mol^{-1}$ | $\sum E^{(2)} = 14.77$ kcal $mol^{-1}$ |
| Sum of repulsion energy | [10] $\sum E_{rep} = 67.02$ kcal $mol^{-1}$ | $\sum E_{rep} = 128.12$ kcal $mol^{-1}$ |
| Sum of heat of formation | [11] $\sum\Delta H_f = -1865.16$ kcal $mol^{-1}$ | $\sum\Delta H_f = -1858.97$ kcal $mol^{-1}$ |

donors through HB interactions influence on properties of systems. Sum of stabilizing energy values for the $Lp_{(Oa)}$ to $\sigma^*_{(Hb-Oc)}$ in the PTX-F127 systems is rather larger than that for the PTX-Lignin structures. Also, complexes with larger $E^{(2)}$ values have fairly larger BE values. The nature of hydrogen bond interplays in the current complexes is attractive. The energy decomposition analyses prove that the exchange energies are main components of the interaction energies. Additionally, the total repulsion energy values in the PTX-F127 complexes are lesser than those in the PTX-Lignin structures. The semi-empirical computations demonstrate that the $\Delta H_f$ values of the PTX-F127 systems are more negative than the PTX-Lignin structures. Also, systems with larger binding energy values have relatively more negative heats of formation

## Data availability

Raw data may be made available on request.

## Statement of usage of artificial intelligence

No usage of AI was carried out.

## Ethical approval

Not applicable (no patients, animal or cells were used in this manuscript).

## CRediT authorship contribution statement

**Pouya Karimi:** Writing – original draft, Visualization, Software, Investigation, Conceptualization. **Mahdiye Poorsargol:** Writing – original draft, Software. **Abbas Rahdar:** Writing – original draft, Supervision, Resources, Methodology, Conceptualization. **Francesco Baino:** Writing – review & editing, Validation.

## Declaration of competing interest

The authors declare that they have no known competing financial interests or personal relationships that could have appeared to influence the work reported in this paper.

## Funding

The authors appreciate the University of Zabol. The Grant number is IR-UOZ-GR-9923 for the current work.

## References

[1] A.K. Singla, A. Garg, D. Aggarwal, Int. J. Pharm.: 235 (2002) 179.
[2] P. Chowdhury, P.K. Nagesh, E. Hatami, J. Colloid. Interface. Sci 535 (2019) 133.
[3] J. Kitayama, H. Ishigami, Yamaguchi, H. Yamashita, Sh. Emoto, Sh. Kaisaki, T. Watanabe, Ann. Surg. Oncol 21 (2014) 539.
[4] L. Della Corte, F. Barra, V. Foreste, P. Giampaolino, G. Evangelisti, S. Ferrero, G. Bifulco, Expert. Opin. Pharmacother.: 21 (2020) 663.
[5] P. Ma, R. Mumper, J. nanomed. nanotechnol. 4 (2013) 1000164.
[6] D. Pooja, H. Kulhari, M. Kuncha, Sh.S. Rachamalla, D.J. Adams, V. Bansal, R. Sistla, Mol. Pharm 13 (2016) 3903.
[7] A. Rahdar, M.R. Hajinezhad, H. Hamishekar, A. Ghamkhari, G.Z. Kyzas, Polym. Bull. 1 (2020) 1.
[8] A. Rahdar, H. Beyzaei, F. Askari, G.Z. Kyzas, Appl. Phys. A: 126 (2020) 1.
[9] A. Rey-Rico, J. Frisch, J.K. Venkatesan, G. Schmitt, I. Rial-Hermida, P. Taboada, A. Concheiro, H. Madry, C. Alvarez-Lorenzo, M. Cucchiarini, ACS. Appl. Mater. Interfaces 32 (2016) 20600.
[10] M. Ali Aboudzadeh, E. Mehravar, M. Fernandez, L. Lezama, R. Tomovska, ACS. Omega 3 (2018) 10999.
[11] A. Rahdar, M. Almasi-Kashi, A.M. Khan, M. Aliahmad, A. Salimi, M. Guettari, H.E. G. Kohne, J. Mol. Liq.: 252 (2018) 506.
[12] S. Sargazi, M.R. Hajinezhad, M. Barani, A. Rahdar, Sh. Shahraki, P. Karimi, M. Cucchiarini, M. Khatami, S. Pandey, J. Mol. Liq 338 (2021) 116625.
[13] A. Rahdar, M.R. Hajinezhad, S. Sargazi, M. Bilal, M. Barani, P. Karimi, G.Z. Kyzas, Life. Sci 270 (2021) 119146.
[14] R. Basak, R. Bandyopadhyay, Langmuir 29 (2013) 4350.
[15] A.O. Nornoo, H. Zheng, L.B. Lopes, B. Johnson-Restrepo, K. Kannan, R. Reed, Eur. J. Pharm. Biopharm.: 71 (2009) 310.
[16] A.O. Nornoo, D.S.L. Chow, Int. J. Pharm.: 349 (2008) 117.
[17] M.A. James-Smith, D. Shekhawat, S. Cheung, B.M. Moudgil, D.O. Shah, J. Surfactants. Deterg 11 (2008) 237.
[18] M.V. Neacsu, I. Matei, M. Micutz, T. Staicu, A. Precupas, V.T. Popa, A. Salifoglou, G. Ionita, J. Phys. Chem. B: 120 (2016) 4258.
[19] X. Meng, J. Liu, X. Yu, J. Li, X. Lu, T. Shen, Sci. Rep 7 (2017) 2964.
[20] H. Wang, G.R. Williams, J. Wu, J. Wu, S. Niu, X. Xie, S. Li, L.M. Zhu, Int. J. Pharm 559 (2019) 289.
[21] A. Rahdar, P. Hasanein, M. Bilal, H. Beyzaei, G.Z. Kyzas, Life. Sci 276 (2021) 119420.
[22] S. Sargazi, M.R. Hajinezhad, M. Barani, M. Mukhtar, A. Rahdar, F. Baino, P. Karimi, S. Pandey, Appl. Scinces 11 (2021) 3006.
[23] A. Rahdar, M.R. Hajinezhad, S. Sargazi, M. Barani, P. Karimi, B. Velasco, P. Taboada, S. Pandey, Z. Bameri, S. Zarei, J. Mol. Liq 346 (2022) 118271.
[24] H. Li, ACS. Sustain. Chem. Eng 4 (2016) 1946.
[25] P. Figueiredo, Biomaterials 121 (2017) 97.
[26] K. Pathania, S.P. Sah, D.B. Salunke, M. Jain, A.K. Yadav, V.G. Yadav, S.V. Pawar, Int. J. Biol. Macromol 229 (2023) 684.
[27] E. Chiani, A. Beaucamp, Y. Hamzeh, M. Azadfallah, A. Thanusha, M.N. Collins, Int. J. Biol. Macromol.: 224 (2023) 1196.
[28] N. Chen, L.A. Dempere, Z. Tong, ACS. Sustain. Chem. Eng 4 (2016) 5204.
[29] M.H. Sipponen, H. Lange, C. Crestini, A. Henn, M. Österberg, ChemSusChem 12 (2019) 2039.
[30] A. Rahdar, S. Sargazi, M. Barani, Sh. Shahraki, F. Sabir, M.Ali Aboudzadeh, Polym. (Basel) 13 (2021) 641.
[31] L. Martínez, R. Andrade, E.G. Birgin, J.M. Martínez, J. Comput. Chem.: 30 (2009) 2157.
[32] M. Stroet, B. Caron, K.M. Visscher, D.P. Geerke, A.K. Malde, A.E. Mark, Automated Topology Builder version 3.0: prediction of solvation free enthalpies in water and hexane, J. Chem. Theory. Comput 14 (2018) 5834.
[33] N. Schmid, A.P. Eichenberger, A. Choutko, S. Riniker, M. Winger, A.E. Mark, W. F. Van Gunsteren, Eur. Biophys. J. 40 (2011) 843.
[34] T. Darden, D. York, L. Pedersen, J. Chem. Phys. 98 (1993) 10089.
[35] G. Bussi, D. Donadio, M. Parrinello, J. Chem. Phys. 126 (2007) 14101.
[36] M. Parrinello, A. Rahman, J. Appl. Phys 52 (1981) 7182.
[37] H. Bekker, H.J.C. Berendsen, E.J. Dijkstra, S. Achterop, R. Vondrumen, D. Vanderspoel, A. Sijbers, H. Keegstra, M.K.R. Renardus, in: 4th Int. Conf. Comput. Phys. (PC 92), World Scientific Publishing, 1993, pp. 252–256.
[38] M.J. Frisch, G.W. Trucks, H.B. Schlegel, G.E. Scuseria, M.A. Robb, J.R. Cheeseman, G. Scalmani, V. Barone, B. Mennucci, G.A. Petersson, H. Nakatsuji, M. Caricato, X. Li, H.P. Hratchian, A.F. Izmaylov, J. Bloino, G. Zheng, J.L. Sonnenberg, M. Hada, M. Ehara, K. Toyota, R. Fukuda, J. Hasegawa, M. Ishida, T. Nakajima, Y. Honda, O. Kitao, H. Nakai, T. Vreven, J.A. Montgomery Jr., J.E. Peralta, F. Ogliaro, M. Bearpark, J.J. Heyd, E. Brothers, K.N. Kudin, V.N. Staroverov, R. Kobayashi, J. Normand, K. Raghavachari, A. Rendell, J.C. Burant, S.S. Iyengar, J. Tomasi, M. Cossi, N. Rega, J.M. Millam, M. Klene, J.E. Knox, J.B. Cross, V. Bakken, C. Adamo, J. Jaramillo, R. Gomperts, R.E. Stratmann, O. Yazyev, A.J. Austin, R. Cammi, C. Pomelli, J.W. Ochterski, R.L. Martin, K. Morokuma, V.G. Zakrzewski, G.A. Voth, P. Salvador, J.J. Dannenberg, S. Dapprich, A.D. Daniels, O. Farkas, J. B. Foresman, J.V. Ortiz, J. Cioslowski, D.J. Fox, Gaussian 09, Revision A.02, Gaussian, Inc., Wallingford CT, 2009.
[39] R.F.W. Bader, Atoms in Molecules: A Quantum Theory, Oxford University Press, Oxford, 1990.
[40] A.E. Reed, L.A. Curtiss, F.J. Weinhold, Chem. Rev 88 (1998) 899.
[41] E.D. Glendening, A.E. Reed, J.E. Carpenter, F. Weinhold, NBO Version 3.1, Gaussian Inc., Pittsburgh, 2003.
[42] M.J.S. Dewar, E.G. Zoebisch, E.F. Healy, J. Am. Chem. Soc. 107 (1985) 3902.
[43] N. Jirofti, M. Poorsargol, F. Sarhaddi, A. Jahani, J. Kadkhoda, F. Kalalinia, A. Rahdar, A. Cambón, P. Taboada, Eur. Polym. J.: 196 (2023) 112228.
[44] P. Chowdhury, P.K. Nagesh, E. Hatami, S. Wagh, N. Dan, M.K. Tripathi, S. Khan, B. B. Hafeez BB, B. Meibohm, S.C. Chauhan, M. Jaggi, M.M. Yallapu, J. Colloid. Interface. Sci 535 (2019) 133.
[45] M.J.S. Phipps, Th. Fox, Ch.S. Tautermann, Ch.K Skylaris, Chem. Soc. Rev 44 (2015) 3177.